HIGHLIGHTS OF A NEW GROUND-BASED, HOURLY GLOBAL LIGHTNING CLIMATOLOGY

BY KATRINA S. VIRTS, JOHN M. WALLACE, MICHAEL L. HUTCHINS, AND ROBERT H. HOLZWORTH

The ground-based World Wide Lightning Location Network (WWLLN) provides unprecedented sampling of lightning frequency, providing a basis for climatologies that resolve diurnal as well as seasonal variations.

Much of the rain that falls in the tropics is associated with deep cumulus convection (Houze 1993, chapter 7, hereafter H93). The clouds exhibit a characteristic life cycle with newly formed, buoyant convective cells consisting of air that has been lifted to its level of free convection in the lower troposphere and begins to ascend freely, drawing on the convective available potential energy (CAPE) inherent in the conditionally unstable midtroposphere (H93). Within an hour or so, the growing cells encounter the stably stratified tropical tropopause transition layer (~12 km; Highwood and Hoskins 1998; Gettelman and de F. Forster 2002), whereupon they spread out to form much longer lived "anvils," in which the air continues to rise but much more slowly (H93). Over the tropics as a whole, roughly half the rain falls as heavy but short-lived showers from the updrafts in convective cells and the other half falls more gently in mesoscale rain areas formed by spreading anvil clouds (Schumacher and Houze 2003). Convective cells originating over the oceans tend to be of moderate intensity with most updraft velocities less than 10 m s^{-1}, whereas those originating over land when the buoyancy of the boundary layer air is enhanced by daytime heating may have updraft velocities up to 15 m s^{-1} or more (Stith et al. 2004), which is strong enough to induce the rates of charge separation required to produce lightning (Zipser and Lutz 1994). Hence, the frequency of occurrence of lightning serves as a proxy for the frequency of occurrence of vigorous updrafts over land and ocean as well as associated phenomena, such as flash floods (Tapia et al. 1998).

Conditionally unstable lapse rates in the midtroposphere are a necessary condition for vigorous convection, but in order to realize the CAPE inherent in the temperature stratification, it is necessary to have sufficient low-level convergence to lift the stably stratified boundary layer air up to its level of free convection (H93). In the tropics, where synoptic-scale

AFFILIATIONS: VIRTS AND WALLACE—Department of Atmospheric Sciences, University of Washington, Seattle, Washington; HUTCHINS AND HOLZWORTH—Department of Earth and Space Sciences, University of Washington, Seattle, Washington
CORRESPONDING AUTHOR: Katrina Virts, Department of Atmospheric Sciences, University of Washington, 408 ATG Bldg., Box 351640, Seattle, WA 98195-1640
Email: kvirts@washington.edu

The abstract for this article can be found in this issue, following the table of contents.
DOI:10.1175/BAMS-D-12-00082.1

A supplement to this article is available online (10.1175/BAMS-D-12-00082.2)

In final form 29 January 2013

disturbances are generally weak, land–sea breezes and mountain–valley wind regimes forced by the diurnal cycle in low-level heating are the dominant mechanism for producing the required lifting, for example, as discussed in Kikuchi and Wang (2008). Daytime heating of the boundary layer air over land can greatly increase the CAPE that can be realized if there is sufficient lifting to trigger convection. It follows that lightning frequency should be strongly modulated by the diurnal cycle and, indeed, it has been shown to be so in numerous regional studies in different parts of the world (e.g., Petersen et al. 1996; Pinto et al. 1999; Collier et al. 2006).

In contrast with the predominantly diurnally forced thunderstorms in the tropics, thunderstorms and heavy precipitation in the extratropics are known to occur in association with migrating synoptic-scale cyclones (Pessi and Businger 2009), but they still occur preferentially over certain favored regions. During winter, cyclones tend to form in the lee of mountain ranges, such as the Andes (Streten and Troup 1973) and Rockies (Zishka and Smith 1980), and over the western oceanic boundary currents and propagate eastward across the oceans, forming so-called storm tracks of enhanced cyclone activity (Hoskins and Valdes 1990). Wintertime cyclones are also observed over the Mediterranean Sea (Alpert et al. 1990).

Until recently, lightning climatologies have been based on station data or local lightning networks, most of which are regional or national in scope. Global satellite-based lightning monitoring began in the 1970s (Turman 1978, and references therein; Orville and Spencer 1979), and statistically significant lightning climatologies became available with the development of the Optical Transient Detector (OTD) and the Lightning Imaging Sensor (LIS; Christian et al. 2000). Datasets derived from these measurements have been used to construct annual-mean and seasonal lightning climatologies (Christian et al. 1999, 2003) and to investigate tropical-mean diurnal lightning variability (Liu and Zipser 2008).

In this paper, we show highlights of a global lightning climatology based on the ground-based World Wide Lightning Location Network (WWLLN, see http://wwlln.net), which has been in operation since 2004. The WWLLN and LIS datasets are described in the "Data" section, and a comparison of the climatological distribution of lightning detected by each sensor is presented in the "TRMM LIS versus WWLLN annual-mean lightning climatologies" section. Seasonal and diurnal variations in lightning frequency observed by WWLLN are discussed in the "Seasonal dependence" section and the "Diurnal dependence" section, respectively, followed by the "Conclusions" section.

DATA. The WWLLN network consists of 68 sensors, as of October 2012 (sensor locations are shown in Fig. 1), that monitor very low-frequency (VLF) radio waves for lightning sferics. The network uses a time of group arrival technique (Dowden et al. 2002) on the detected sferic waveforms to locate lightning to within ~5 km and <10 μs (Abarca et al. 2010). Comparisons between lightning observations from WWLLN and regional networks indicate that the global detection efficiency of WWLLN is ~10% (Rodger et al. 2006, 2009; Abarca et al. 2010; Connaughton et al. 2010; Hutchins et al. 2012a) of all strokes, which is sufficient to enable WWLLN to detect almost all lightning-producing storms (Jacobson et al. 2006).

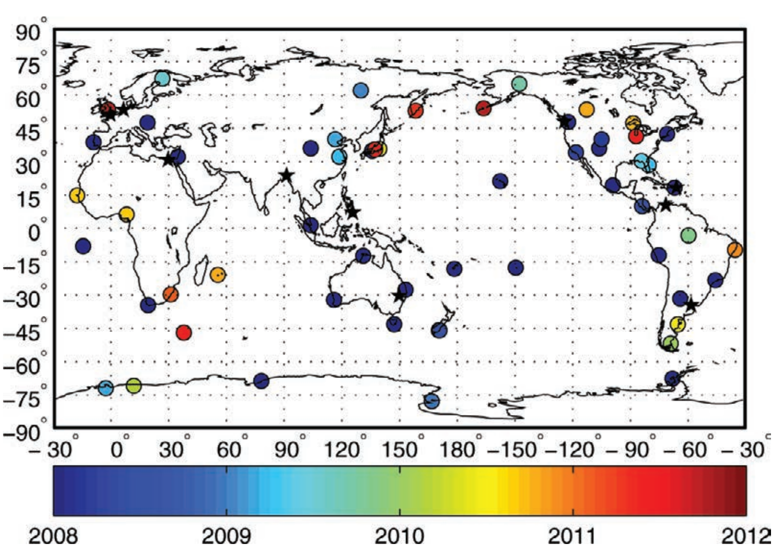

Fig. 1. Location of WWLLN sensors, color coded according to the date each was established. Stations established prior to 2008 are shown in dark blue; black stars indicate stations established 2012–present.

Abarca et al. (2010) compared WWLLN hourly lightning frequency over the United States with observations from the National Lightning Detection Network (NLDN) and found some marked differences. The agreement was somewhat better when comparing subsets of each climatology corresponding to strokes with strong peak currents, but the dfferences were still large enough that they expressed reservations concerning the ability of WWLLN to capture the diurnal cycle. In addition, attenuation of the VLF waves used by WWLLN to locate lightning strokes is strongest during daytime (Hutchins et al. 2012b), introducing a possible bias toward detecting more nighttime than daytime lightning. However, we will show in the "Diurnal dependence" section that the WWLLN hourly climatology is generally consistent with prior ground-based studies and with our understanding of the processes that cause lightning to vary systematically with time of day.

OTD was launched with the *MicroLab-1* satellite in April 1995 into a 70° inclination orbit (Christian et al. 2003), and LIS is carried on the Tropical Rainfall Measuring Mission (TRMM) satellite, which was launched in 1997 into a 35° inclination orbit (Christian et al. 1999). In this study, we make use of lightning climatologies based on ~13 years of LIS and ~5 years of OTD observations. Annual-mean and hourly mean climatologies are available at 0.5° and 2.5° spatial resolution, respectively. TRMM also carries a Precipitation Radar (PR) and a Visible and Infrared Scanner (VIRS). TRMM rainfall observations are supplemented with data from other satelliteborne microwave imagers and infrared sensors to generate the gridded TRMM 3B42 dataset (Huffman et al. 2007), which is available at three-hourly temporal resolution and 0.25° spatial resolution.

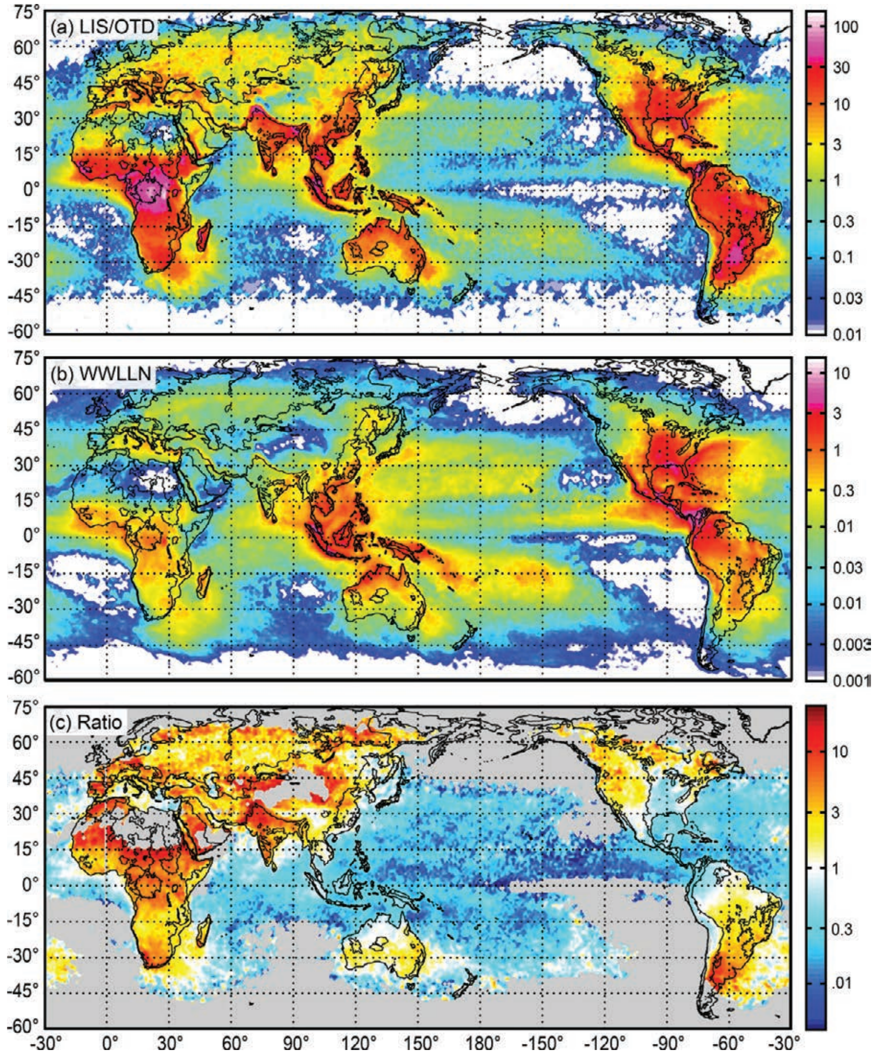

Fig. 2. Annual-mean frequency of occurrence of lightning from (a) LIS/OTD (flashes km^{-2} yr^{-1}) and (b) WWLLN (strokes km^{-2} yr^{-1}). (c) Ratio of LIS/OTD flashes to WWLLN strokes, scaled by the mean of each dataset (gray shading indicates either no LIS/OTD lightning flashes or WWLLN lightning stroke frequency <0.01 km^{-2} yr^{-1}; see text for details). All fields have been averaged on a 1° × 1° grid. Black contours indicate the 500-m elevation.

Given the complexity of lightning, interpreting the differences between lightning climatologies based on observations from different instruments or networks is not straightforward. LIS/OTD and WWLLN rely on fundamentally different detection methods. WWLLN receivers detect sferics that have propagated in the Earth–ionosphere waveguide and are fully captured within a 1-ms window at each station (Dowden et al. 2002). In contrast, LIS and OTD are optical staring imagers that detect momentary changes in cloud brightness caused by lightning; optical transients that are similarly located in space and time are grouped into events referred to as flashes (Christian et al. 2000). WWLLN preferentially detects strong cloud-to-ground strokes, and it rarely detects and locates multiple strokes within a single flash because the dispersed waveforms overlap or because there is a large difference in total radiated energy (Rodger et al. 2004, 2005; Jacobson et al. 2006). Hence, the number of individual strokes is relatively close to the number of flashes detected by WWLLN. It follows that comparing climatologies of WWLLN strokes and LIS/OTD flashes should be informative even though, strictly speaking, strokes and flashes are different phenomena. Further specifics on WWLLN may be found in the supplemental material (available online at http://dx.doi.org.10.1175/BAMS-D-12-00082.2) and in the peer-reviewed articles listed online (at http://wwlln.net/publications).

TRMM LIS VERSUS WWLLN ANNUAL-MEAN LIGHTNING CLIMATOLOGIES. The frequency of occurrence of lightning, as detected by WWLLN during the years 2008–11, is compared with LIS/OTD observations in Figs. 2a,b. The two climatologies are qualitatively similar, both showing a concentration of lightning over major tropical continents—Africa, southeastern Asia and Australasia, and Central and South America—with strong gradients near the coastlines and features that bear a strong relationship to the underlying topography. For example, lightning is frequently observed in the central United States between the Rocky and Appalachian Mountains. Both lightning climatologies differ substantially from the TRMM rainfall climatology shown in Fig. 3a, in which the maxima are located over the oceanic "warm pool" covering the equatorial Indian and western Pacific Oceans and in the region of the intertropical convergence zone (ITCZ). Lightning also tends to be more geographically focused than rainfall: in the WWLLN and LIS climatologies for the tropical belt (30°N–30°S), half the lightning strokes are observed in 8% of the area, whereas half the rain falls over 22% of the area (not shown). These distinctions illustrate the importance of daytime heating of the atmospheric boundary layer over land in creating the conditions required for the initiation of intense convection, as discussed earlier.

The color bars in Figs. 2a,b have been chosen so as to emphasize the similarities between the LIS/OTD and WWLLN lightning climatologies. Differences between the two climatologies are illustrated in Fig. 2c, which shows the pointwise ratio of lightning frequency reported by LIS/OTD and WWLLN. For display purposes, this ratio was multiplied by a scaling factor—the global-mean WWLLN lightning frequency divided by the global-mean LIS/OTD lightning frequency—so that values <1 indicate proportionally more WWLLN lightning, and vice versa, relative to their respective global means. With a few notable exceptions (e.g., over the Maritime Continent and the southeastern United States), LIS/OTD reports proportionally more lightning over land and less over the oceans than WWLLN. Because WWLLN's detection efficiency is higher for lightning strokes with higher peak currents (Rodger et al. 2009), the land–sea contrasts in Fig. 2c may reflect a tendency for lightning strokes over the oceans to be more powerful than over land. This tendency was previously noted by Rudlosky and Fuelberg (2010) in an analysis of the mean peak currents in negative cloud-to-ground flashes reported by the NLDN. The unevenness of the spacing of the WWLLN stations (Fig. 1) also contributes to the observed differences between the LIS/OTD and WWLLN climatologies. For example, it is evident from Fig. 2c that the LIS

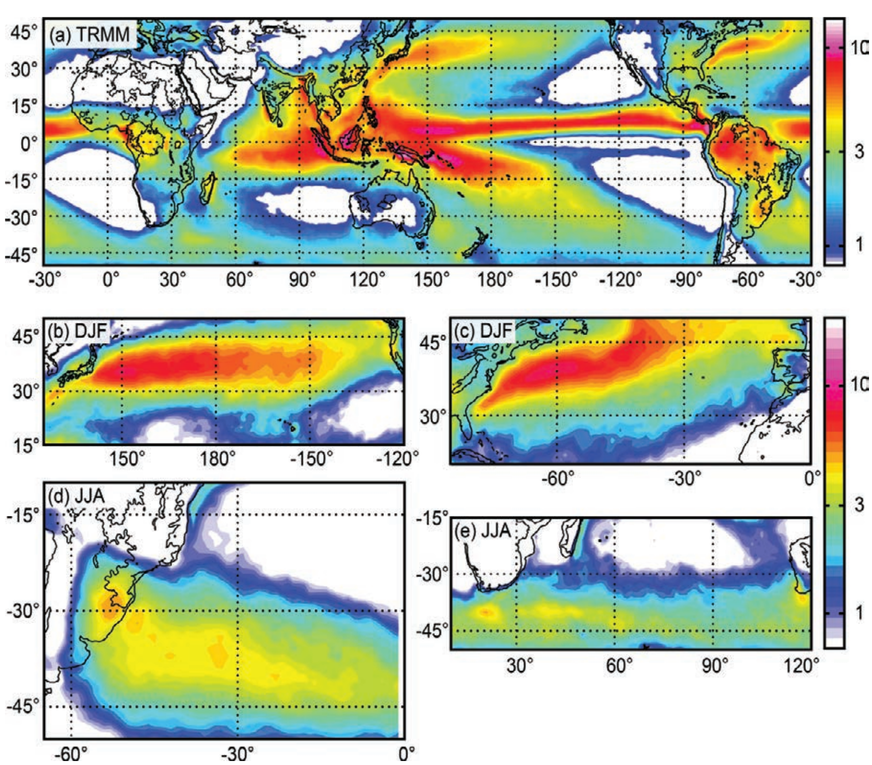

Fig. 3. TRMM (a) annual-mean and (b)–(e) seasonal-mean precipitation (mm day^{-1}; 1° × 1° resolution). Black contours indicate the 500-m elevation.

lightning climatology places relatively greater emphasis on the maxima in lightning frequency in areas such as Africa and the Himalayas, where WWLLN's detection efficiency is lower (Hutchins et al. 2012a). Further analysis of lightning stroke energy, particularly over the eastern United States, is ongoing.

For broad regional comparisons between lightning frequency over different continental regions, such as Central America versus India, LIS is clearly the definitive dataset for latitudes up to ~35°. The advantage of WWLLN is that it samples continuously over the whole globe, whereas LIS and OTD sample only when the satellite passes overhead (~0.1% of the time over much of the tropics; Christian et al. 1999, 2003). When detection efficiency [~10% for WWLLN, as discussed in the "Data" section, and ~80%–90% for LIS, according to Boccippio et al. (2002)] is taken into account, WWLLN samples ~100 times as many strokes/flashes per year as LIS. The difference in the number of samples has little effect on the appearance of the annual-mean lightning climatologies shown in Fig. 2, but it becomes a more important consideration when considering how finely the data can be disaggregated by synoptic situation and/or by time of day.

In the "Seasonal dependence" and "Diurnal dependence" sections, we describe some regional, WWLLN-based seasonal and diurnal lightning climatologies that reveal, with an unprecedented level of detail, how the occurrence of vigorous convection is maximized in the extratropical wintertime storm tracks and in the tropics, where it is shaped by the underlying topography and land–sea distribution. The selected images for prescribed seasons and times of day shown in the text are complemented by 12-month animations of the climatological-mean seasonal cycle and 24-h animations of the climatological-mean diurnal cycle in the online supplement for this article (available at http://dx.doi.org.10.1175/BAMS-D-12-00082.2), and by a more extensive selection of animations on the WWLLN website.

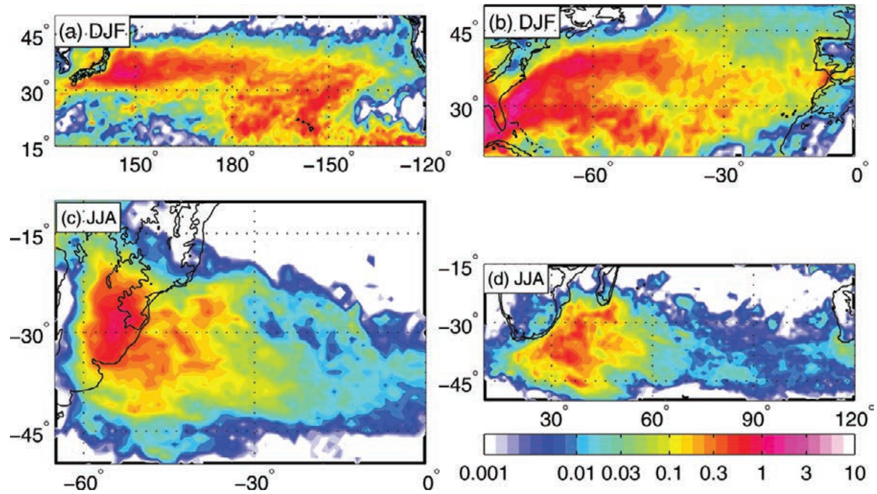

Fig. 4. WWLLN seasonal-mean lightning stroke frequency ($km^{-2}\ yr^{-1}$; 1° × 1° resolution) during (a),(b) Dec–Feb (DJF) and (c),(d) Jun–Aug (JJA). Black contours indicate the 500-m elevation.

SEASONAL DEPENDENCE. WWLLN lightning and TRMM precipitation over the northern Pacific and Atlantic Oceans during Northern Hemisphere winter are shown in Figs. 4a,b and in Figs. 3b,c, respectively; corresponding maps for the southern Atlantic and Indian Oceans during Southern Hemisphere winter are shown in Figs. 4c,d and Figs. 3d,e. The zonally elongated precipitation bands observed in each ocean basin between ~30° and 45° latitude are associated with the wintertime storm tracks, as described earlier, with the North Atlantic storm track appearing to veer poleward at the downstream end. Vigorous convection is also found in the storm tracks, as evidenced by the corresponding lightning bands in Fig. 4. The lightning maxima lie along, or a few degrees equatorward of, the axes of maximum rainfall, and suggestions of secondary east–west-oriented lightning maxima are evident at subtropical latitudes to the west of Hawaii and to the southeast of Bermuda. Based on data from LIS and the Pacific Lightning Detection Network, Pessi and Businger (2009) concluded that much of the lightning in the storm tracks occurs in thunderstorms embedded in the cold fronts of midlatitude cyclones. During winter, both lightning densities and rainfall rates are larger over the oceans than over land. Strong gradients are observed along the coasts and over warm western boundary currents. Over Argentina, wintertime cyclone development takes place in the lee of the Andes (Streten and Troup 1973), and the lightning and precipitation maxima both begin over Argentina (Figs. 3d, 4c). Over both the South Atlantic and the southern Indian Oceans, the lightning tends to be concentrated on the western side of the storm track, where sea surface temperatures are higher. Global, monthly-mean lightning animations based on WWLLN and LIS/OTD observations are in the supplemental material (available at http://dx.doi.org.10.1175/BAMS-D-12-00082.2).

Cyclonic disturbances also produce thunderstorms over the Mediterranean during the local winter season (Defer et al. 2005). Both lightning and precipitation are more frequent over the warmer sea than over the colder European landmass (Figs. 5a,b), in agreement with previous studies based on data from local lightning networks (Altaratz et al. 2003; Katsanos et al. 2007). Lightning gradients along the northern and eastern coasts of the Mediterranean and Adriatic are particularly sharp, where there is steep terrain near the coast. Composite analysis (not shown) shows that southwesterly flow is observed during days of frequent lightning along the northeastern Adriatic coast. The low-level instability produced by colder air moving over the warmer Mediterranean waters can create a favorable environment for thunderstorm development in the absence of cyclones (Altaratz et al. 2003). In contrast, during Northern Hemisphere summer, lightning and precipitation are most frequent over the warmer European continent (Figs. 5c,d; Chronis 2012), where thunderstorms form over the Alps, the Pyrenees, and the mountains of the Balkan Peninsula. Lightning occurrence over the latter region was examined by Kotroni and Lagouvardos (2008) using an experimental lightning network.

DIURNAL DEPENDENCE. The diurnal cycle of lightning over the Maritime Continent, the central Andes, and the African Great Lakes is summarized in Figs. 6–8 in terms of maps of the climatological frequency of occurrence of lightning during selected segments of the day. These summary maps and the animations in the supplemental material (available at http://dx.doi.org.10.1175/BAMS-D-12-00082.2) reveal the following characteristics of the diurnal variability.

- In response to the diurnal cycle in incoming solar radiation, convection begins around local noon over inland regions with relatively flat terrain such as the Amazon basin (Fig. 7) and parts of central Africa (Fig. 8). Over these regions, lightning occurs most frequently during afternoon and early evening, with a late afternoon peak, and least frequently during the morning. Rainfall over the tropical continents exhibits a diurnal cycle with a similarly timed peak (Kikuchi and Wang 2008). Diurnal lightning variability is smaller in Argentina (Fig. 7), where long-lived mesoscale convective systems (MCSs; Nesbitt et al. 2000) produce nighttime lightning.
- During sunny days, warm air rises along mountain slopes as an anabatic wind, or "valley breeze." Thunderstorms form over the steep terrain just west of the crest of the Andes during late morning and shift to the east of the crest by ~1600 LT, where they linger into early evening. The influence of valley breezes is also evident in the intense thunderstorms that begin in the early afternoon along the western slopes of the Mitumba and Virunga Mountains of central Africa and produce maximum lightning ~1900 LT (Fig. 8; Jackson et al. 2009). Similarly, afternoon and early evening lightning is frequently observed over the slopes of the mountains of the Maritime Continent (Fig. 6).
- At night, cooling air drains down from the mountains into the valleys as a katabatic wind, or "mountain breeze," inducing weak ascent over the lower terrain that is augmented where valleys of adjacent tributaries converge. Lightning occurs on the valley floor to the east of the Andes (Fig. 7), where nocturnal convection tends to be organized into mesoscale convective complexes (Bendix et al. 2009), but not on the west side of the Andes, where the boundary layer air is much drier. Adjacent to the Andes, lightning is observed most frequently just before midnight and persists into the morning of the next day. In some cases, nighttime lightning

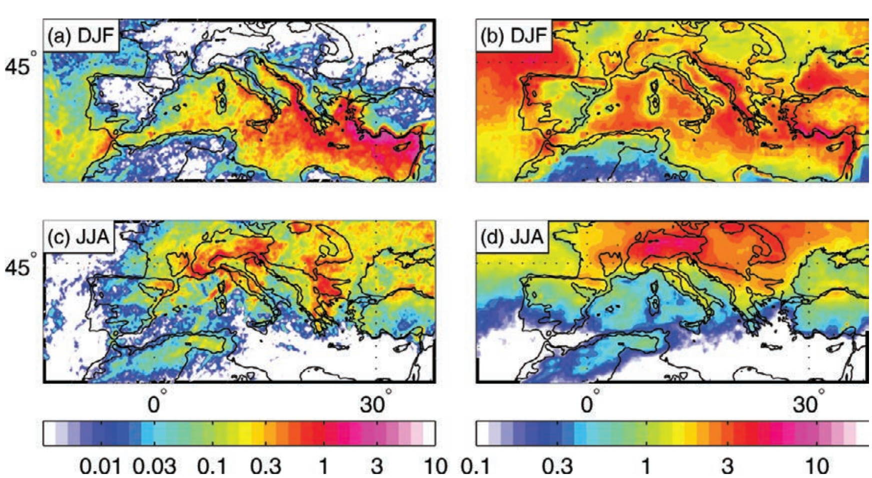

Fig. 5. (a),(c) WWLLN lightning stroke frequency (km^{-2} yr^{-1}) and (b),(d) TRMM 3B42 precipitation (mm day^{-1}; both at 0.25° × 0.25° resolution) during (a),(b) DJF and (c),(d) JJA. Black contours indicate the 500-m elevation.

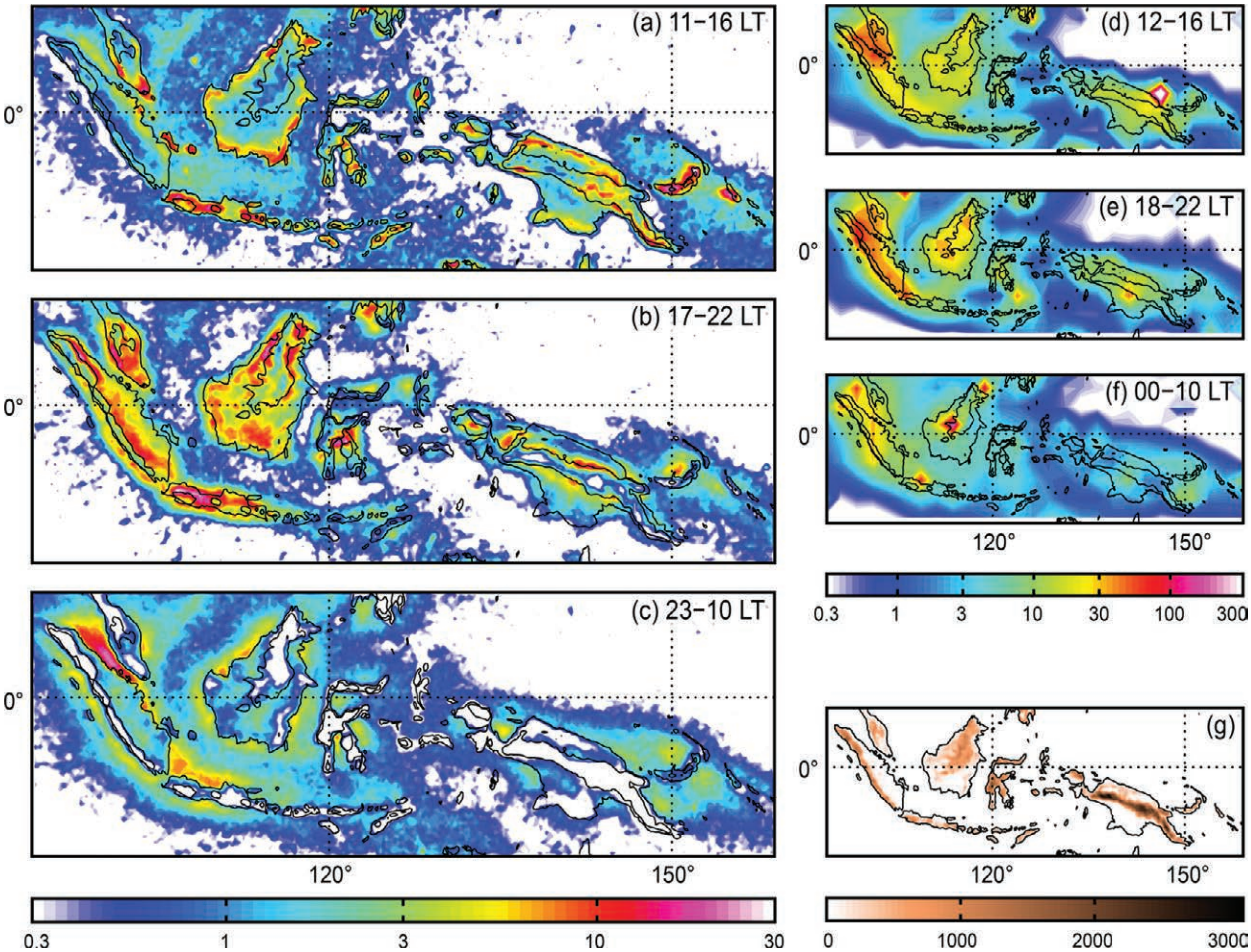

Fig. 6. (a)–(c) WWLLN lightning stroke frequency (km^{-2} yr^{-1}; hourly, 0.25° × 0.25° resolution) and (d)–(f) LIS/OTD lightning flash frequency (km^{-2} yr^{-1}; two hourly, 2.5° × 2.5° resolution) for indicated time intervals during all months. Local time given for Singapore. Black contours indicate the 500-m elevation. (g) Elevation (m).

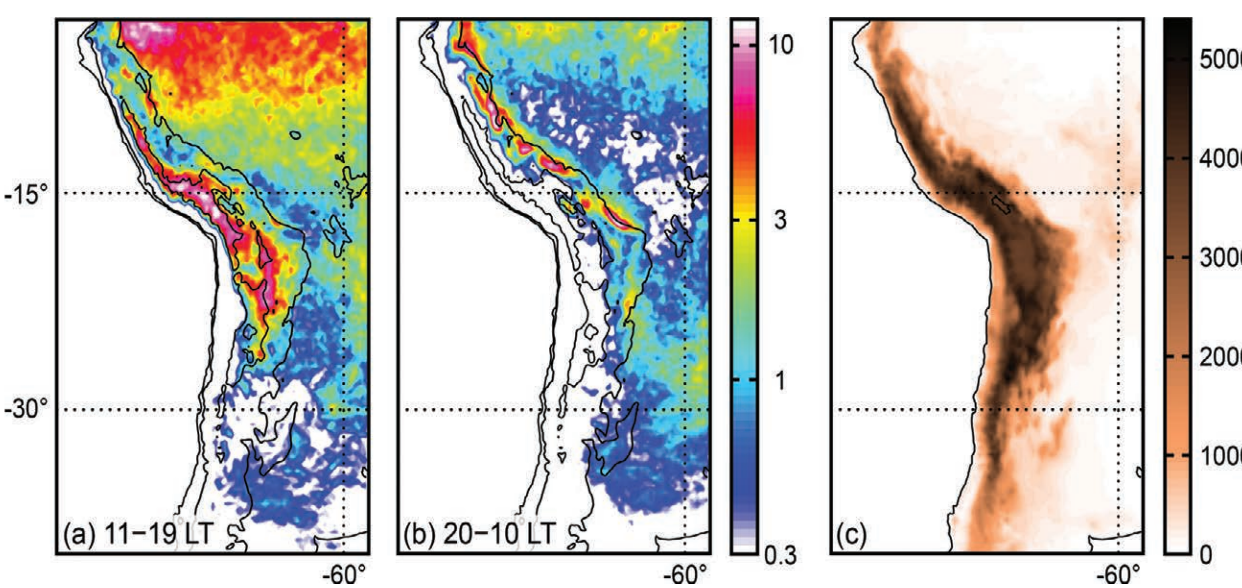

Fig. 7. (a),(b) WWLLN lightning stroke frequency (km^{-2} yr^{-1}; 0.25° × 0.25° resolution) over the central Andes for indicated time intervals during Nov–Mar. Local time given for Lima, Peru. Black contours indicate the 500- and 4000-m elevation. (c) Elevation (m).

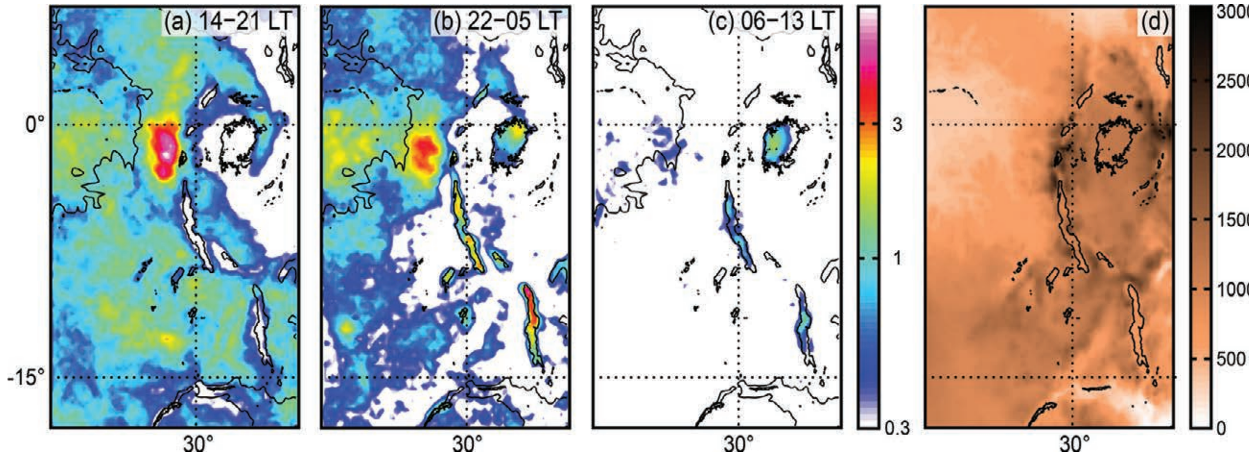

Fig. 8. As in Fig. 7, but for tropical Africa for all months. Local time given for Kampala, Uganda.

frequencies are similar in magnitude to the daytime maxima over the mountain slopes. Over the Maritime Continent, the mountains are free of lightning at night, while thunderstorms linger over the surrounding lowlands (Fig. 6).

- Strong diurnal variations in lightning occurrence are also observed near coastlines. On sunny mornings, land surfaces, with their smaller heat capacities, warm up rapidly, resulting in strong temperature and pressure contrasts along coastlines that drive onshore winds, or "sea breezes." Over the Maritime Continent, convection begins around noon as the sea-breeze fronts develop and intensify as they propagate inland during the afternoon, with peak lightning frequencies around 1600–1700 LT (Fig. 6). Locally, lightning is enhanced where convex coastlines result in sea-breeze convergence, for example, over parts of Borneo. Most small islands experience brief afternoon lightning maxima approximately three to five hours in duration and become lightning free by early evening, while thunderstorms over larger islands persist into the evening. Similar behavior has been noted in precipitation duration (Qian 2008). Where mountains and coastlines are in close proximity, sea breezes and valley breezes can act in concert to produce strong afternoon and evening convection (Mahrer and Pielke 1977).
- At night, when the boundary layer over land cools, coastal circulation patterns reverse, resulting in "land breezes." Thunderstorms begin ~2000 LT over Lakes Malawi and Kivu in central Africa and an hour or two later over Lakes Victoria, Tanganyika, and Albert (Fig. 8). Land breezes, enhanced by katabatic winds from the surrounding terrain (Savijärvi and Järvenoja 2000), strengthen and converge over the lakes through the night, and lightning is observed most frequently at ~0400–0500 LT. Over Lake Victoria, the lightning maximum shifts from the northeastern part of the lake to the southwestern part by morning; similar behavior was observed by Hirose et al. (2008) based on TRMM precipitation data. No corresponding shift is observed over the other lakes.

Near the Maritime Continent, the nocturnal convection regime is more complex. Locally, land breezes and mountain breezes result in offshore winds, and areas with concave coastlines exhibit enhanced nighttime lightning (Fig. 6). In addition, features in the animations (available at http://dx.doi.org.10.1175/BAMS-D-12-00082.2, and at http://wwlln.net/climate) that resemble gravity waves propagate out of the regions of afternoon convection and appear to trigger thunderstorms over the coastal waters, as in the numerical simulations of Mapes et al. (2003). The daytime lightning over the western slopes of the mountains of Sumatra moves offshore in late afternoon into a region of weakening convective inhibition (Wu et al. 2009), propagates southwestward, and weakens after sunrise the following day, in agreement with the description of Mori et al. (2004) based on TRMM rainfall data. Strong convection and frequent lightning occur between 2200 and 1200 LT in the Strait of Malacca, where land breezes from Sumatra and the Malay Peninsula converge (Fujita et al. 2010). Elsewhere, such as along the northern coast of New Guinea, a separate line of thunderstorms forms along the coast just before midnight and moves offshore in the early morning hours. By morning, each of the major islands is surrounded by a ring of lightning, consistent with the TRMM rainfall climatology of Kikuchi and Wang (2008).

Diurnal lightning maps for the Maritime Continent based on the LIS/OTD climatology are shown in Fig. 6. The WWLLN and LIS/OTD climatologies are similar in some respects—for example, both indicate that lightning is more frequent over the major islands during the afternoon and evening than during the morning. However, the spatial resolution of the LIS/OTD climatology is too coarse to fully resolve features such as the morning lightning maximum in the Strait of Malacca. Hour-by-hour time series of WWLLN lightning for three areas of interest, including the Strait of Malacca, are included in the supplemental material (available at http://dx.doi.org.10.1175/BAMS-D-12-00082.2).

The discussion in this paper has focused on diurnal lightning variability in the climatological mean or, for the Andes, the extended local summer season. Phenomena such as the monsoons (Kandalgaonkar et al. 2003), El Niño–Southern Oscillation (Hamid et al. 2001), and the Madden–Julian Oscillation (Kodama et al. 2006) also modulate lightning occurrence and, likely, its diurnal cycle (Virts et al. 2013).

CONCLUSIONS. TRMM LIS and WWLLN are the only existing lightning datasets that provide global coverage. LIS provides a well-calibrated tropical lightning climatology that already extends for over 14 years. WWLLN has been in operation for only a few years, but it offers the possibility of monitoring lightning frequency over the entire globe with sample sizes two orders of magnitude larger than is feasible with LIS, as evidenced by the comparison in Fig. 6. The two datasets are highly complementary. The Geostationary Operational Environmental Satellite–R Series (GOES-R) satellite, scheduled for launch in 2015, will carry aboard a lightning sensor that will provide continuous coverage over the North American sector, thereby providing a certain degree of redundancy in the lightning measurements in that sector.

In this paper we have shown some highlights from a seasonal and diurnal cycle lightning climatology constructed from WWLLN data binned hourly and in 0.25° × 0.25° grid boxes. Though no single lightning climatology can be said to be definitive, the WWLLN lightning climatology appears to be consistent with in situ rainfall observations and with the TRMM rainfall climatology, and it provides a plausible representation of how the frequency of deep cumulus convection varies over the course of the day in the vicinity of coastlines and orography. Indeed, most of the features of the seasonal and diurnal cycles derived from WWLLN and the mechanisms that give rise to them have been known, or at least hinted at, for decades. What is new is the unprecedented ability to view the diurnal cycle in lightning from a global perspective with high spatial resolution. Although we have not illustrated it here, the large sample size of WWLLN data makes it possible to refine the analysis in order to investigate how the diurnal cycle in lightning changes with season and in response to day-to-day variations in wind patterns and vertical profiles of temperature and moisture. Such analyses will be useful for refining our understanding of the environmental conditions that give rise to intense convection and for validating numerical models that attempt to simulate the statistics of intense convection in a realistic setting.

ACKNOWLEDGMENTS. The authors thank the editor and three anonymous reviewers for their helpful comments and suggestions. This work was supported by the National Science Foundation under Grant ATM 0812802 and by NOAA under Contract NA10OAR4320148 AM62. Lightning location data were provided by WWLLN (http://wwlln.net), a collaboration among over 50 universities and institutions. The LIS/OTD climatologies were obtained from NASA's Global Hydrology and Climate Center (http://ghcc.msfc.nasa.gov/). TRMM rainfall data were obtained from NASA's Goddard Earth Sciences Data and Information Services Center (http://mirador.gsfc.nasa.gov/).

REFERENCES

Abarca, S. F., K. L. Corbosiero, and T. J. Galarneau Jr., 2010: An evaluation of the Worldwide Lightning Location Network (WWLLN) using the National Lightning Detection Network (NLDN) as ground truth. *J. Geophys. Res.,* **115,** D18206, doi:10.1029/2009JD013411.

Alpert, P., B. U. Neeman, and Y. Shay-El, 1990: Climatological analysis of Mediterranean cyclones using ECMWF data. *Tellus,* **42A,** 65–77.

Altaratz, O., Z. Levin, Y. Yair, and B. Ziv, 2003: Lightning activity over land and sea on the eastern coast of the Mediterranean. *Mon. Wea. Rev.,* **131,** 2060–2070.

Bendix, J., K. Trachte, J. Cermak, R. Rollenbeck, and T. Nauß, 2009: Formation of convective clouds at the foothills of the tropical eastern Andes (south Ecuador). *J. Appl. Meteor. Climatol.,* **48,** 1682–1695.

Boccippio, D. J., W. J. Koshak, and R. J. Blakeslee, 2002: Performance assessment of the Optical Transient Detector and Lightning Imaging Sensor. Part I: Predicted diurnal variability. *J. Atmos. Oceanic Technol.,* **19,** 1318–1332.

Christian, H. J., and Coauthors, 1999: The Lightning Imaging Sensor. *Proc. 11th Int. Conf. on Atmospheric Electricity,* Guntersville, AL, International Commission on Atmospheric Electricity, 726–729.

——, R. J. Blakeslee, S. J. Goodman, and D. M. Mach, 2000: Algorithm Theoretical Basis Document (ATBD) for the Lightning Imaging Sensor (LIS). NASA, 53 pp. [Available online at http://eospso.gsfc.nasa.gov/sites/default/files/atbd/atbd-lis-01.pdf.]

——, and Coauthors, 2003: Global frequency and distribution of lightning as observed from space by the Optical Transient Detector. *J. Geophys. Res.,* **108,** 4005, doi:10.1029/2002JD002347.

Chronis, T. G., 2012: Preliminary lightning observations over Greece. *J. Geophys. Res.,* **117,** D03113, doi:10.1029/2011JD017063.

Collier, A. B., A. R. W. Hughes, J. Lichtenberger, and P. Steinbach, 2006: Seasonal and diurnal variation of lightning activity over southern Africa and correlation with European whistler observations. *Ann. Geophys.,* **24,** 529–542.

Connaughton, V., and Coauthors, 2010: Associations between Fermi Gamma-Ray Burst Monitor terrestrial gamma ray flashes and sferics from the World Wide Lightning Location Network. *J. Geophys. Res.,* **115,** A12307, doi:10.1029/2010JA015681.

Defer, E., K. Lagouvardos, and V. Kotroni, 2005: Lightning activity in the eastern Mediterranean region. *J. Geophys. Res.,* **110,** D24210, doi:10.1029/2004JD005710.

Dowden, R. L., J. B. Brundell, and C. J. Rodger, 2002: VLF lightning location by time of group arrival (TOGA) at multiple sites. *J. Atmos. Sol. Terr. Phys.,* **64,** 817–830.

Fujita, M., F. Kimura, and M. Yoshizaki, 2010: Morning precipitation peak over the Strait of Malacca under a calm condition. *Mon. Wea. Rev.,* **138,** 1474–1486.

Gettelman, A., and P. M. de F. Forster, 2002: A climatology of the tropical tropopause layer. *J. Meteor. Soc. Japan,* **80,** 911–924.

Hamid, E. Y., Z.-I. Kawasaki, and R. Mardiana, 2001: Impact of the 1997–98 El Niño event on lightning activity over Indonesia. *Geophys. Res. Lett.,* **28,** 147–150.

Highwood, E. J., and B. J. Hoskins, 1998: The tropical tropopause. *Quart. J. Roy. Meteor. Soc.,* **124,** 1579–1604.

Hirose, M., R. Oki, S. Shimizu, M. Kachi, and T. Higashiuwatoko, 2008: Finescale diurnal rainfall statistics refined from eight years of TRMM PR data. *J. Appl. Meteor. Climatol.,* **47,** 544–561.

Hoskins, B. J., and P. J. Valdes, 1990: On the existence of storm tracks. *J. Atmos. Sci.,* **47,** 1854–1864.

Houze, R. A., Jr., 1993: *Cloud Dynamics*. Academic Press, 573 pp.

Huffman, G. J., and Coauthors, 2007: The TRMM Multisatellite Precipitation Analysis (TMPA): Quasi-global, multiyear, combined-sensor precipitation estimates at fine scales. *J. Hydrometeor.,* **8,** 38–55.

Hutchins, M. L., R. H. Holzworth, J. B. Brundell, and C. J. Rodger, 2012a: Relative detection efficiency of the World Wide Lightning Location Network. *Radio Sci.,* **47,** RS6005, doi:10.1029/2012RS005049.

——, ——, C. J. Rodger, and J. B. Brundell, 2012b: Far-field power of lightning strokes as measured by the World Wide Lightning Location Network. *J. Atmos. Oceanic Technol.,* **29,** 1102–1110.

Jackson, B., S. E. Nicholson, and D. Klotter, 2009: Mesoscale convective systems over western equatorial Africa and their relationship to large-scale circulation. *Mon. Wea. Rev.,* **137,** 1272–1294.

Jacobson, A. R., R. Holzworth, J. Harlin, R. Dowden, and E. Lay, 2006: Performance assessment of the World Wide Lightning Location Network (WWLLN), using the Los Alamos Sferic Array (LASA) as ground truth. *J. Atmos. Oceanic Technol.,* **23,** 1082–1092.

Kandalgaonkar, S. S., M. I. R. Tinmaker, J. R. Kulkarni, and A. Nath, 2003: Diurnal variation of lightning activity over the Indian region. *Geophys. Res. Lett.,* **30,** 2022, doi:10.1029/2003GL018005.

Katsanos, D., K. Lagouvardos, V. Kotroni, and A. Argiriou, 2007: Combined analysis of rainfall and lightning data produced by mesoscale systems in the central and eastern Mediterranean. *Atmos. Res.,* **83,** 55–63.

Kikuchi, K., and B. Wang, 2008: Diurnal precipitation regimes in the global tropics. *J. Climate,* **21,** 2680–2696.

Kodama, Y.-M., M. Tokuda, and F. Murata, 2006: Convective activity over the Indonesian Maritime Continent during CPEA-I as evaluated by lightning activity and Q1 and Q2 profiles. *J. Meteor. Soc. Japan,* **84A,** 133–149.

Kotroni, V., and K. Lagouvardos, 2008: Lightning occurrence in relation with elevation, terrain slope, and vegetation cover in the Mediterranean. *J. Geophys. Res.,* **113,** D21118, doi:10.1029/2008JD010605.

Liu, C., and E. J. Zipser, 2008: Diurnal cycles of precipitation, clouds, and lightning in the tropics from 9 years of TRMM observations. *Geophys. Res. Lett.,* **35,** L04819, doi:10.1029/2007GL032437.

Mahrer, Y., and R. A. Pielke, 1977: The effects of topography on sea and land breezes in a two-dimensional numerical model. *Mon. Wea. Rev.,* **105,** 1151–1162.

Mapes, B. E., T. T. Warner, and M. Xu, 2003: Diurnal patterns of rainfall in northwestern South America. Part III: Diurnal gravity waves and nocturnal convection offshore. *Mon. Wea. Rev.,* **131,** 830–844.

Mori, S., and Coauthors, 2004: Diurnal land–sea rainfall peak migration over Sumatera Island, Indonesian Maritime Continent, observed by TRMM satellite and intensive rawinsonde soundings. *Mon. Wea. Rev.,* **132,** 2021–2039.

Nesbitt, S. W., E. J. Zipser, and D. J. Cecil, 2000: A census of precipitation features in the tropics using TRMM: Radar, ice scattering, and lightning observations. *J. Climate,* **13,** 4087–4106.

Orville, R. E., and D. W. Spencer, 1979: Global lightning flash frequency. *Mon. Wea. Rev.,* **107,** 934–943.

Pessi, A. T., and S. Businger, 2009: Relationships among lightning, precipitation, and hydrometeor characteristics over the North Pacific Ocean. *J. Appl. Meteor. Climatol.,* **48,** 833–848.

Petersen, W. A., S. A. Rutledge, and R. E. Orville, 1996: Cloud-to-ground lightning observations from TOGA COARE: Selected results and lightning location algorithms. *Mon. Wea. Rev.,* **124,** 602–620.

Pinto, I. R. C. A., O. Pinto Jr., R. M. L. Rocha, J. H. Diniz, A. M. Carvalho, and A. Cazetta Filho, 1999: Cloud-to-ground lightning in southeastern Brazil in 1993: 2. Time variations and flash characteristics. *J. Geophys. Res.,* **104** (D24), 31 381–31 387.

Qian, J.-H., 2008: Why precipitation is mostly concentrated over islands in the Maritime Continent. *J. Atmos. Sci.,* **65,** 1428–1441.

Rodger, C. J., J. B. Brundell, R. L. Dowden, and N. R. Thomson, 2004: Location accuracy of long distance VLF lightning location network. *Ann. Geophys.,* **22,** 747–758.

——, ——, and ——, 2005: Location accuracy of VLF World-Wide Lightning Location (WWLL) network: Post-algorithm upgrade. *Ann. Geophys.,* **23,** 277–290.

——, S. Werner, J. B. Brundell, E. H. Lay, N. R. Thomson, R. H. Holzworth, and R. L. Dowden, 2006: Detection efficiency of the VLF World-Wide Lightning Location Network (WWLLN): Initial case study. *Ann. Geophys.,* **24,** 3197–3214.

——, J. B. Brundell, R. H. Holzworth, E. H. Lay, N. B. Crosby, T.-Y. Huang, and M. J. Rycroft, 2009: Growing detection efficiency of the World Wide Lightning Location Network. *Coupling of Thunderstorms and Lightning Discharges to Near-Earth Space: Proceedings of the Workshop,* N. B. Crosby, T.-Y. Huang, and M. J. Rycroft, Eds., *AIP Conference Proceedings,* Vol. 1118, American Institute of Physics, 15–20, doi:10.1063/1.3137706.

Rudlosky, S. D., and H. E. Fuelberg, 2010: Pre- and postupgrade distributions of NLDN reported cloud-to-ground lightning characteristics in the contiguous United States. *Mon. Wea. Rev.,* **138,** 3623–3633.

Savijärvi, H., and S. Järvenoja, 2000: Aspects of the fine-scale climatology over Lake Tanganyika as resolved by a mesoscale model. *Meteor. Atmos. Phys.,* **73,** 77–88.

Schumacher, C., and R. A. Houze Jr., 2003: Stratiform rain in the tropics as seen by the TRMM precipitation radar. *J. Climate,* **16,** 1739–1756.

Stith, J. L., J. A. Haggerty, A. Heymsfield, and C. A. Grainger, 2004: Microphysical characteristics of tropical updrafts in clean conditions. *J. Appl. Meteor.,* **43,** 779–794.

Streten, N. A., and A. J. Troup, 1973: A synoptic climatology of satellite observed cloud vortices over the Southern Hemisphere. *Quart. J. Roy. Meteor. Soc.,* **99,** 56–72.

Tapia, A., J. A. Smith, and M. Dixon, 1998: Estimation of convective rainfall from lightning observations. *J. Appl. Meteor.,* **37,** 1497–1509.

Turman, B. N., 1978: Analysis of lightning data from the DMSP satellite. *J. Geophys. Res.,* **83** (C10), 5019–5024.

Virts, K. S., J. M. Wallace, M. L. Hutchins, and R. H. Holzworth, 2013: Diurnal lightning variability over the Maritime Continent: Impact of low-level winds, cloudiness, and the MJO. *J. Atmos. Sci.,* in press, doi:10.1175/JAS-D-13-021.1.

Wu, P., M. Hara, J.-I. Hamada, M. D. Yamanaka, and F. Kimura, 2009: Why a large amount of rain falls over the sea in the vicinity of western Sumatra island during nighttime. *J. Appl. Meteor. Climatol.,* **48,** 1345–1361.

Zipser, E. J., and K. R. Lutz, 1994: The vertical profile of radar reflectivity of convective cells: A strong indicator of storm intensity and lightning probability? *Mon. Wea. Rev.,* **122,** 1751–1759.

Zishka, K. M., and P. J. Smith, 1980: The climatology of cyclones and anticyclones over North America and surrounding ocean environs for January and July, 1950–77. *Mon. Wea. Rev.,* **108,** 387–401.